



## A novel fluoride selective optical chemosensor based on internal charge transfer signaling

Sabir H. Mashraqui<sup>a,\*</sup>, Rupesh Betkar<sup>a</sup>, Mukesh Chandiramani<sup>a</sup>, David Quinonero<sup>b</sup>, Antonio Frontera<sup>b</sup>

<sup>a</sup> Department of Chemistry, University of Mumbai, Vidyanaagari, Santacruz-E, Mumbai 400098, India

<sup>b</sup> Department de Química, Universitat de les Illes Balears, Palma de Mallorca 07122, Balears, Spain

### ARTICLE INFO

#### Article history:

Received 14 October 2009

Revised 11 November 2009

Accepted 13 November 2009

Available online 20 November 2009

### ABSTRACT

A new internal charge transfer probe, NAPH-1, synthesized by incorporating photoemittive naphthalimide core with an acidic imidazolium ring, offers highly selective colorimetric and ratiometric 'off-on' signaling for targeting F<sup>-</sup>, while Cl<sup>-</sup>, Br<sup>-</sup>, I<sup>-</sup>, HSO<sub>4</sub><sup>-</sup>, SCN<sup>-</sup>, AcO<sup>-</sup>, and NO<sub>3</sub><sup>-</sup> do not appreciably perturb the photophysical properties of the probe even at relatively higher concentrations than the F<sup>-</sup>. Deprotonation of the imidazolium ring, supported by the <sup>1</sup>H NMR and theoretical studies, seems to cause the spectral modulations.

© 2009 Elsevier Ltd. All rights reserved.

Anion recognition constitutes an area of fundamental importance because of the key roles anions play in a range of chemical and biological processes.<sup>1</sup> In biological systems, anion interactions primarily occur via hydrogen bonding at the specific H-donor sites on proteins. By analogy, the design criteria for artificial optical anion sensors during past years have typically relied upon anion interactions with different neutral and cationic H-donor receptors, while the optical transductions have been expressed by exploiting different photophysical protocols which include photoinduced electron transfer, metallo-ligand charge transfer, internal charge transfer (ICT) mechanisms, and excimer formation.<sup>2</sup>

For a number of medical, clinical, and environment-related issues, the selective and practical detection of fluoride ion are a subject of major current interest.<sup>3</sup> With this perspective, many optical fluoride sensors featuring either 'off-on'<sup>4</sup> or 'on-off'<sup>5</sup> type responses and with or without additional colorimetric sensing have been recently investigated. Though, not as extensively studied, however by far the most appealing fluoride ion sensors are those offering dual, colorimetric, and ratiometric 'off-on' type optical readouts.<sup>6</sup>

Since the ICT probes experience both ground and excited state perturbations upon analyte binding,<sup>7</sup> the ICT protocol can be used to harness dual colorimetric-fluoregenic sensors. On this ground, we have incorporated a chromogenic naphthalimide core with the acidic imidazolium ring to access a novel ICT chemosensor, NAPH-1. It may be noted that though the photoemittive naphthalimide<sup>8</sup> and the acidic imidazolium<sup>9</sup> moieties have in the past been separately used as a part of chemosensors, to the best of our knowledge, their joint incorporation in the sensor design is unprecedented.

The design concept behind NAPH-1 is based on the understanding that the  $\pi$ -deficient naphthalimide ring, by virtue of its electron-withdrawing nature would boost the acidity of the imidazolium ring. In the event of strong anion binding, the forming negative charge on the imidazolium ring would induce the ICT character into the system. Consequently, significant optical modulations by ways of optical spectral shift and intensity variation can be expected in the probe upon anion complexations.

The synthesis of NAPH-1 was achieved by condensing 4-nitro-1, 8-naphthalic anhydride **1** with *p*-methoxybenzylamine **2** in refluxing AcOH to afford naphthalimide **3** (Scheme 1). Heating the latter with imidazole in dry DMF gave imidazole-substituted naphthalimide **4**. Quarternization of **4** with CH<sub>3</sub>I in anhydrous CH<sub>3</sub>CN gave iodide salt **5** which upon anion exchange with an excess of Mg(ClO<sub>4</sub>)<sub>2</sub> in CH<sub>3</sub>CN afforded NAPH-1 as a pale yellow solid in good overall yield.

Addition of 100 equiv (1.5 × 10<sup>-3</sup> M) of the tetra-*n*-butylammonium salt (TBA) of F<sup>-</sup> exhibited remarkable spectral variations, exhibiting a new red-shifted absorption band at 585 nm (extinction coefficient,  $\epsilon_m$  5.08 × 10<sup>4</sup> M<sup>-1</sup> cm<sup>-1</sup>), and the shift of the LE band from 335 to 360 nm.

As depicted in Fig. 1, the longer wavelength absorption at 585 nm is attributable to the ICT transition, which originates as a consequence of the F<sup>-</sup> binding interaction with the imidazolium receptor. In contrast, addition of up to 1000 equiv of TBA salts of Cl<sup>-</sup>, Br<sup>-</sup>, I<sup>-</sup>, HSO<sub>4</sub><sup>-</sup>, SCN<sup>-</sup>, and NO<sub>3</sub><sup>-</sup> did not detectably alter the UV-vis profile of NAPH-1, while exposing the probe to 1000 equiv of the acetate ion induced a red-shifted band around 585 nm, but with a drastically low  $\epsilon_m$  value of 1.3 × 10<sup>2</sup> M<sup>-1</sup> cm<sup>-1</sup>.

The spectrophotometric titration of NAPH-1 (1.5 × 10<sup>-5</sup> M) with TBAF (0–1.5 × 10<sup>-3</sup> M) is depicted in Figure 2. The inset depicts a graphical representation of the steady changes in the

\* Corresponding author. Tel.: +91 22 26526091; fax: +91 22 26528547.  
E-mail address: [sh\\_mashraqui@yahoo.com](mailto:sh_mashraqui@yahoo.com) (S.H. Mashraqui).



sponse was also induced by the  $\text{AcO}^-$  at 10 times higher than the limiting concentration of  $\text{F}^-$ .

Thus, in the presence of  $1.2 \times 10^{-3}$  M of  $\text{AcO}^-$ , the emission intensity measured at 438 nm was enhanced only by 4-fold and moreover, under this condition, the probe's emission band at 373 nm was only partially diminished. Job's plot derived from the fluorimetric titration with  $\text{F}^-$  suggested 1:1 binding interaction and the association constant,  $\log K$  calculated using the nonlinear curve fitting method was found to be 2.49. For the case of  $\text{AcO}^-$ , the  $\log K$  was determined to be 0.46, which is nearly two orders of magnitude lower than that found for the  $\text{F}^-$ . The  $\log K_s$  for other anions could not be reliably calculated due to insignificant interactions.

The superior affinity of the  $\text{F}^-$  was validated by a competitive fluorescence experiment. No significant variations in the emission profile of the probe containing  $1.2 \times 10^{-4}$  M of  $\text{F}^-$  were detected upon adding  $1.2 \times 10^{-3}$  M each of  $\text{Cl}^-$ ,  $\text{Br}^-$ ,  $\text{I}^-$ ,  $\text{HSO}_4^-$ ,  $\text{SCN}^-$ ,  $\text{AcO}^-$ , and  $\text{NO}_3^-$ . These findings bear out that  $\text{Cl}^-$ ,  $\text{Br}^-$ ,  $\text{I}^-$ ,  $\text{HSO}_4^-$ ,  $\text{SCN}^-$ ,  $\text{AcO}^-$ , and  $\text{NO}_3^-$  do not or only scarcely perturb the excited states of NAPH-1. The detection limit of  $\text{F}^-$ , determined fluorimetrically, was found to be  $3.86 \times 10^{-6}$  M, which is lower among numerous reported fluoride sensors.<sup>4–6</sup> The emission intensity ratio,  $I_{438}/I_{373}$  increased linearly with respect to increasing fluoride concentrations. Thus, in addition to the 'naked eye' sensing, the fluorescence ratiometric protocol is available, enhancing the utility of NAPH-1 for the fluoride ion detection.

The strong binding interaction of  $\text{F}^-$  with NAPH-1 was also corroborated by the  $^1\text{H}$  NMR experiment (Fig. 4). Addition of 5 equiv of TBAF resulted in the broadening and downfield shift of the imidazolium C(2)–H from 9.1 to 15.2 ppm, whereas the N–Me group moved upfield from 4.1 to 2.7 ppm. These results imply the development of a high degree of negative charge at the C-2 position of the imidazolium ring. We assume that the electron-withdrawing naphthalimide ring increases the acidity of the imidazolium ring, thereby facilitating the interaction by the strongly basic fluoride ion.

To understand the anion binding, we performed DFT calculations at the level of RI-BP86/def-TZVP in DMSO solvent. To facilitate the calculations, we replaced the *p*-methoxybenzene by a methyl group. In the optimized structure (Fig. 5), the torsional angle of the naphthyl-imidazolium bond in the protonated form is 66 degrees (COSMO computation). Calculations show that only  $\text{F}^-$  is able to withdraw the C(2)–H hydrogen with a distance of approximately 1.6 Å. Furthermore, the torsional angle is reduced to 50 degrees in one conformation and to 51 degrees in another conformation upon  $\text{F}^-$  interaction. The ca. 15 degrees reduction in torsional angle reflects increasing conjugative tendency between the  $\pi$ -deficient naphthalimide ring and the deprotonated imidazolium ring. This phenomenon appears to be responsible for the dramatic effects observed in the optical properties of the probe in the presence of fluoride ion.

Though the optimized geometries of the selected complexes of the selected anions  $\text{Cl}^-$ ,  $\text{Br}^-$ , and  $\text{AcO}^-$  do show the formation of H-bonding, however the acidic C(2)–H remain attached to the imidazolium ring. The computed binding energies for the selected anions both in the gas phase and in the DMSO solvent were found in the order  $\text{F}^- \gg \text{AcO}^- > \text{Cl}^- > \text{Br}^-$ , implying the superior binding affinity of the fluoride ion.

The theoretically calculated  $^1\text{H}$  NMR values of the imidazolium C(2)–H of the probe and its fluoride complex were found to be 7.49 and 12.5 ppm, respectively. Although the absolute value ( $\Delta\delta = 5.01$  ppm) is lower than the experimental one ( $\Delta\delta = 6.1$  ppm), the theoretical downfield shift prediction is acceptable. This result gives reliability to the theoretical model, especially since chemical shifts are sensitive to the geometry of the compound.

Though our theoretical work seems to indicate deprotonation, the available optical and  $^1\text{H}$  NMR data do not allow distinction between the strong C(2)–H... $\text{F}^-$  interaction and the extreme case of full deprotonation by the strongly basic fluoride ion to generate the carbene.<sup>13</sup> Nevertheless, the  $\text{F}^-$  induced ICT process, that is, red shift in the UV–vis spectrum and the high Stokes shift in the ICT emission maximum, can be reasonably reconciled taking into

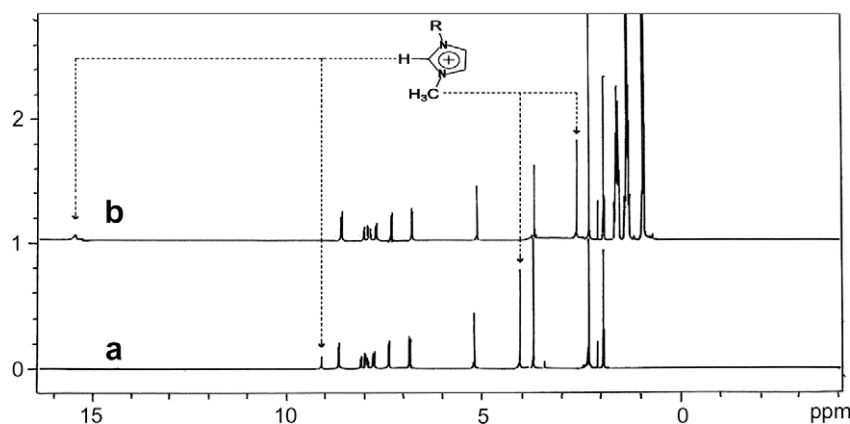


Figure 4.  $^1\text{H}$  NMR spectrum (a) of NAPH-1 and (b) of NAPH-1 + TBAF (5 equiv) in  $\text{DMSO}-d_6$ .

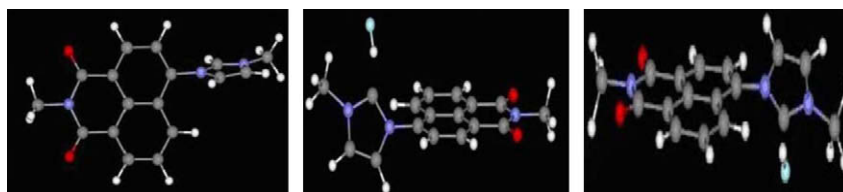


Figure 5. RI-BP86/def-TZVP optimized structures, right: conformation of *N*-methyl analog of NAPH-1; middle and left: two different conformations involving the  $\text{F}^-$  interaction.

consideration the involvement of either the C(2)–H...F<sup>-</sup> interaction or the nucleophilic carbene.

The excellent selectivity of NAPH-1 toward the F<sup>-</sup> can be attributed to its high basicity which makes it a strong contender to engage the receptor, while its small size should allow an unencumbered access to the imidazolium ring held in a twisted conformation. However, effective interactions with other anions could be precluded or limited due to their lower basicities and/or larger ionic sizes.

To summarize, our strategy of directly attaching a naphthalimide core with an imidazolium receptor has yielded the chemosensor, NAPH-1 as one of the rare examples of the internal charge transfer probes, which delivers dual-mode colorimetric 'naked eye' detection as well as an efficient ratiometric luminescent 'turn-on' sensing for targeting the fluoride ion. Importantly, several other anions, including the commonly interfering AcO<sup>-</sup>, caused none or minimal optical perturbations even at relatively higher concentrations than the fluoride ion. A large downfield shift of the imidazolium C(2)–H confirms the strong binding interaction with the highly basic F<sup>-</sup>. The DFT calculations predict F<sup>-</sup> induced deprotonation as well as reduction in the torsional angle of the probe. The ensuing electronic conjugation between the deprotonated imidazolium ring and the electron deficient naphthalimide ring appears to cause the observed spectral modulations.

### Supplementary data

Experimental details, selected <sup>1</sup>H/<sup>13</sup>C NMR spectra, graph for anion induced emission enhancements, Job's plot, ratiometric graph, competitive fluorescence binding profile, detection limit, and Table for anion binding energies are available. Supplementary data associated with this article can be found, in the online version, at doi:10.1016/j.tetlet.2009.11.050.

### References and notes

- (a) Dietrich, B.; Hosseini, M. W. In *Supramolecular Chemistry of Anions*; Bianchi, A., Bowman-James, K., García-España, E., Eds.; Wiley-VCH: New York, 1997; pp 45–62; (b) Stilbor, I., Ed.; *Anion Sensing*, *Top. Curr. Chem.* **2005**, 255.
- (a) Mániz, R. M.; Sancenón, S. *Chem. Rev.* **2003**, 103, 4419–4476; (b) Sessler, J. L.; Seidel, D. *Angew. Chem., Int. Ed.* **2003**, 42, 5134–5175; (c) Gale, P. A. *Coord. Chem. Rev.* **2003**, 240, 191–221; (d) Suksai, C.; Tuntulani, T. *Chem. Soc. Rev.* **2003**, 32, 192–202.
- (a) Waldbott, G. L. *Clin. Toxicol.* **1981**, 18, 531–541; (b) Matuso, S.; Kiyomiya, K.-i.; Kurebe, M. *Arch. Toxicol.* **1998**, 72, 798–806; (c) Riggs, B. L. *Bone Miner. Res.* **1984**, 2, 366–393.
- (a) Fabbrizzi, L.; Faravelli, H.; Franzese, G.; Licchelli, M.; Perotti, A.; Taglietti, A. *Chem. Commun.* **1998**, 9, 971–972; (b) Galbraith, E.; Fyles, T.; Marken, M. F.; Davidson, M. G.; James, T. D. *Inorg. Chem.* **2008**, 47, 6236–6244; (c) Kim, S. K.; Yoon, J. *Chem. Commun.* **2002**, 2, 770–771; (d) Black, C. B.; Andrioletti, B.; Try, A. C.; Ruiperez, C.; Sessler, J. L. *J. Am. Chem. Soc.* **1999**, 121, 10438–10439; (e) Anzenbacher, P., Jr.; Jursikova, K.; Sessler, J. L. *J. Am. Chem. Soc.* **2000**, 122, 9350–9351; (f) Cho, E. J.; Ryu, B. J.; Lee, Y. J.; Nam, K. C. *Org. Lett.* **2005**, 7, 2607–2609; (g) Xu, Z.; Kim, S.; Kim, H. N.; Han, S. J.; Lee, C.; Kim, J. S.; Qian, X.; Yoon, J. *Tetrahedron Lett.* **2007**, 48, 9151–9154; (h) Duke, R. M.; Gunnlaugsson, T. *Tetrahedron Lett.* **2007**, 48, 8043–8047.
- (a) Lu, H.; Xu, W.; Zhang, D.; Chen, C.; Zhu, D. *Org. Lett.* **2005**, 7, 4629–4632; (b) Lee, J. Y.; Cho, E. J.; Mukamel, S.; Nam, K. C. *J. Org. Chem.* **2004**, 69, 943–950; (c) Xu, G.; Tarr, M. A. *Chem. Commun.* **2004**, 4, 1050–1051; (d) Liu, C.; Qian, X.; Sun, G.; Zhao, L.; Li, Z. *New J. Chem.* **2008**, 32, 472–476; (e) Hudnall, T. W.; Gabbai, F. P. *Chem. Commun.* **2008**, 8, 4596–4597; (f) Panzella, L.; Pezzella, A.; Arzillo, M.; Manini, P.; Napolitano, A.; d'Ischia, M. *Tetrahedron* **2009**, 65, 2032–2036; (g) Swamy, K. M. K.; Lee, Y. J.; Lee, H. N.; Chun, J.; Kim, Y.; Kim, S.-J.; Yoon, J. *J. Org. Chem.* **2006**, 71, 8626–8628; (h) Jose, D. A.; Kumar, D. K.; Ganguly, B.; Das, A. *Org. Lett.* **2004**, 6, 3445–3448; (i) Cho, E. J.; Moon, J. W.; Ko, S. W.; Lee, J. Y.; Kim, S. K.; Yoon, J.; Nam, K. C. *J. Am. Chem. Soc.* **2003**, 125, 12376–12377.
- (a) Kubo, Y.; Yamamoto, M.; Ikeda, M.; Takeuchi, M.; Shinkai, S.; Yamaguchi, S.; Tamao, K. *Angew. Chem., Int. Ed.* **2003**, 42, 2036–2040; (b) Liu, B.; Tian, H. *J. Mater. Chem.* **2005**, 15, 2681–2686; (c) Peng, X.; Wu, Y.; Fan, J.; Tian, M.; Han, K. *J. Org. Chem.* **2005**, 70, 10524–10531; (d) Lin, C.-H.; Selvi, S.; Fang, J.-M.; Chou, P.-T.; Lai, C.-H.; Cheng, Y.-M. *J. Org. Chem.* **2007**, 72, 3537–3542.
- (a) Rotkiewicz, K.; Grabowski, Z. R.; Rettig, W. *Chem. Rev.* **2003**, 103, 3899–4032; (b) Rettig, W. *Angew. Chem., Int. Ed. Engl.* **1986**, 25, 971–988.
- Gunnlaugsson, T.; Glynn, M.; Gillian, M. T.; Paul, E. K.; Frederick, M. P. *Coord. Chem. Rev.* **2006**, 250, 3094–3117.
- Yoon, J.; Kim, S. K.; Singh, N. J.; Kwang, S.; Kim, K. S. *Chem. Soc. Rev.* **2006**, 35, 355–360.
- (a) He, X.; Hu, S.; Liu, K.; Guo, Y.; Xu, J.; Shao, S. *Org. Lett.* **2006**, 8, 333–336; (b) Zhang, X.; Guo, L.; Wu, F.-Y.; Jiang, Y.-B. *Org. Lett.* **2003**, 5, 2667–2670; (c) Kang, J.; Kima, H.-S.; Janga, D.-O. *Tetrahedron Lett.* **2005**, 46, 6079–6082; (d) Thiagarajan, V.; Ramamurthy, P.; Thirumalai, D.; Ramakrishnan, V. T. *Org. Lett.* **2005**, 7, 657–660; (e) Gunnlaugsson, T.; Davis, A. P.; Glynn, M. *Chem. Commun.* **2001**, 1, 2556–2557; (f) Lee, C.; Lee, D. H.; Hong, J.-I. *Tetrahedron Lett.* **2001**, 42, 8665–8669; (g) Gong, W.-T.; Harigae, J.; Seo, J.; Lee, S. S.; Hiratani, K. *Tetrahedron Lett.* **2008**, 49, 2268–2271; (h) Costero, A. M.; Banuls, M. J.; Aurell, M. J.; DeArellano, M. C. R. *J. Inclusion Phenom. Macrocyclic Chem.* **2006**, 54, 61–66.
- (a) Wu, F.-Y.; Li, Z.; Wen, Z.-C.; Zhou, N.; Zhao, Y.-F.; Jiang, Y.-B. *Org. Lett.* **2002**, 4, 3203–3205; (b) Neto, B.-A.-D.; Lopes, A.-S.-A.; Ebeling, G.; Gonc, R.-S.; Costa, V.-E.-U.; Quina, F.-H.; Dupont, J. *Tetrahedron* **2005**, 61, 10975–10982.
- Shiraishi, Y.; Maehara, H.; Sugii, T.; Wang, D.; Hirai, T. *Tetrahedron Lett.* **2009**, 50, 4293–4296.
- Lapis, A.-A.-M.; de Oliveira, L.-F.; Neto, B.-A.-D.; Dupont, J. *Chem. Sus. Chem.* **2008**, 1, 759–762.